Production of intense pulsed beams of highly charged ions from a superconducting electron cyclotron resonance ion source

L. X. Li,[1,2] J. B. Li,[1,*] J. D. Ma,[1] H. Guo,[3] B. Guo,[3] D. Hitz,[1] Y. C. Feng,[1] W. Lu,[1,2] J. W. Guo,[1] X. Fang,[1] R. N. Jin,[1] Y. J. Yuan,[1,2] L. T. Sun,[1,2,†] and H. W. Zhao[1,2]

[1]*Institute of Modern Physics (IMP), Chinese Academy of Sciences, Lanzhou 730000, People's Republic of China*
[2]*School of Nuclear Science and Technology, University of Chinese Academy of Sciences, Beijing 100049, People's Republic of China*
[3]*Gansu Medical Device Inspection and Testing Institute, Lanzhou 730070, People's Republic of China*

(Received 4 March 2022; accepted 23 May 2022; published 16 June 2022)

An experimental study of the afterglow mode was performed with a third generation electron cyclotron resonance ion source, SECRAL-II (Superconducting ECR ion source with Advanced design in Lanzhou No. II), under double frequency heating. The experimental results show that intense pulsed beams of highly charged ions (e.g., 266 eμA of $^{129}Xe^{34+}$ and 169 eμA of $^{129}Xe^{38+}$) could be produced at high frequency (24 + 18 GHz) and high power (~8 kW), even compared with the beam intensity records of SECRAL-II obtained in continuous wave (cw) mode at higher microwave frequency (28 + 18 GHz) and higher power (~10 kW), the gain factor is also up to ~3. Meanwhile, it is found that the afterglow decay time in our study is much longer than that obtained with the second generation ECR ion sources typically operating at 10–18 GHz, and the corresponding peak duration is greater than 2 ms. This study provides a viable solution for heavy ion synchrotron accelerator complex such as High Intensity Heavy Ion Accelerator Facility project that requires intense pulsed beams of highly charged ions with long peak duration.

DOI: 10.1103/PhysRevAccelBeams.25.063402

I. INTRODUCTION

To expand nuclear and related researches into the presently unreachable region and give scientists possibilities to conduct cutting-edge researches in these fields, an international HIAF (High Intensity Heavy Ion Accelerator Facility) project is under construction at Institute of Modern Physics, Chinese Academy of Sciences (IMP) [1]. The general layout of the HIAF complex is shown in Fig. 1, consisting of superconducting electron cyclotron resonance (ECR) ion sources injector, superconducting linear accelerator iLinac, high intensity synchrotron booster ring (BRing), multifunction high-precision synchrotron spectrometer ring (SRing), superconducting radioactive beam line HIAF FRagment Separator (HFRS), and several experimental terminals. As the HIAF features unprecedented high beam intensity, the beam intensity of highly charged ions for BRing is designed up to $\sim 10^{11}$ ppp. Meanwhile, to achieve high injection gain in BRing, the two-plane painting multiturn injection scheme will be applied to inject ~100 turns with a gain factor of 82.5–90.5 [2], which corresponds to an injection time of 1–2 ms. Moreover, the shortest work cycle of BRing for heavy ions is designed to be 374 ms [3], and consequently intense

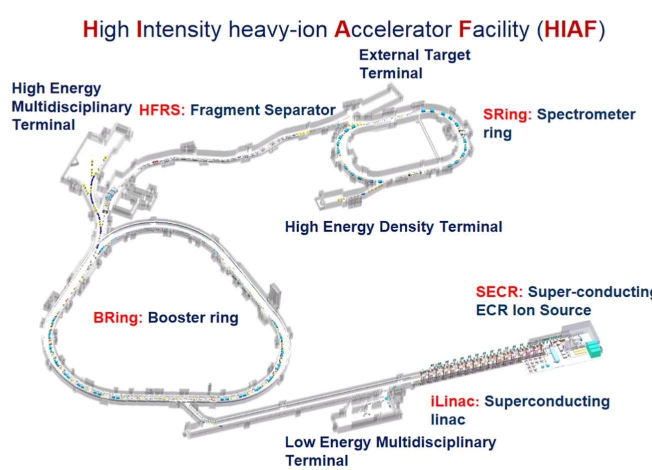

FIG. 1. The general layout of the HIAF complex.

*jiboli@impcas.ac.cn
†sunlt@impcas.ac.cn

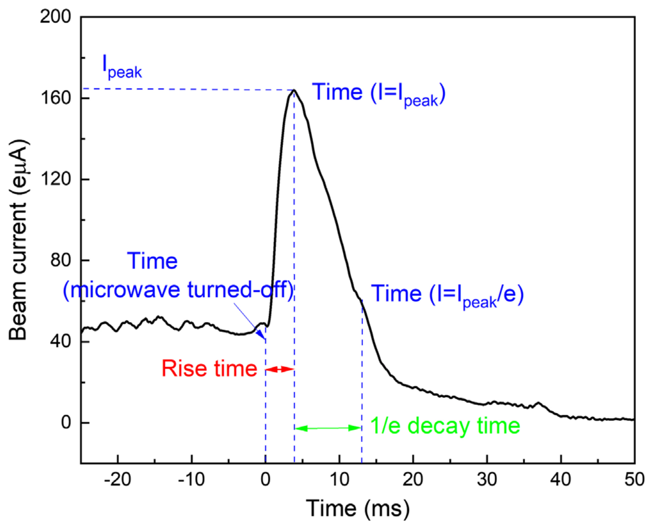

FIG. 2. A typical afterglow waveform and characteristic parameters of Xe^{38+} beams in our experiments.

pulsed beams of highly charged ions produced by the ECR ion source with ≥ 2 ms peak duration and 1–3 Hz repetition rate are needed for HIAF. To fulfill this requirement, in addition to developing the next generation ECR ion source [4], it is important to carry out continued research aiming at the improvement of intense pulsed ion beam production.

Pulsed beam production for an ECR ion source is most commonly achieved by the use of afterglow mode, this mode was first discovered in Grenoble [5] and has been successfully applied at CERN (European Organization for Nuclear Research) [6,7] as a routine operation. Multiple studies [8–11] have shown that the afterglow mode is characterized by a periodic pulsing of the microwave power and by an intense burst of highly charged ions following the switch-off of the microwave power (see Fig. 2). When this power is stopped, the electrons are no more confined and escape from the trap created by the magnetic confinement, and in order to fulfill the plasma electroneutrality, the ions follow the electrons. It is well known that the peak current of highly charged ions during afterglow transient is usually several times higher than that in continuous wave (cw) mode. Moreover, a recent experimental study [12] has demonstrated that the addition of the secondary frequency can significantly enhance and stabilize the extracted beam currents during the afterglow discharge. However, neither the peak beam intensity nor the reported afterglow peak duration (typically less than 1 ms) with today's ECR ion sources [8,12] can meet the HIAF requirement, this motivates us to improve the afterglow performance.

An experimental study [13] carried out on first and second generation ECR ion sources had shown that the decay time of afterglow transient is proportional to the magnetic field strength. And then, with the higher magnetic fields of SECRAL-II, one can expect a longer decay time and peak duration. Meanwhile, since the beam intensity in cw mode of the third generation ECR ion source is always much higher than that of the second generation machine [14], a more intense beam can also be expected when operating a third generation ECR ion source in afterglow mode.

In this article, we present an experimental study of the afterglow mode with a SECRAL-II ion source operated under double frequency heating, i.e., 24 GHz + 18 GHz. The experimental setup and equipment are described in Sec. II; in Sec. III, the experimental results are reported; a discussion about the data is then shown in Sec. IV.

II. EXPERIMENTAL SETUP

SECRAL-II, the ion source used for our experiment is a fully superconducting ECR ion source developed at IMP [15]. This machine is a quasi duplicate of SECRAL ion source [16–18] but has a slightly higher radial field and a larger plasma chamber. The main design parameters of SECRAL-II and SECRAL ion sources are listed in Table I. As a third generation ECR machine, SECRAL-II exhibits high performance in the production of intense highly charged ion beams in cw mode with a number of beam intensity records [19]. The feature structure of SECRAL-II superconducting magnet is to locate the three axial solenoid coils inside the radial sextupole magnet, rather than the typical magnetic structure for most ECR ion sources, which is made of axial solenoid coils surrounding the radial sextupole magnet. For microwave injection into the plasma chamber, a circular waveguide and two WR62 type rectangular waveguides (designed for 24–28 GHz and 14–18 GHz microwave injection, respectively) are inserted axially through the ion source injection system, and the arrangement of the waveguides and other ports at the plasma chamber injection end is shown in Fig. 3.

Since the CPI 28 GHz gyrotron cannot be operated in pulsed mode, in our experiments with double frequency heating, the circular waveguide was connected to a GyCOM 24 GHz gyrotron having a maximum output power of 8 kW, and one of the rectangular waveguides was connected to an 18-GHz klystron amplifier having a

TABLE I. Main design parameters of SECRAL-II and SECRAL ion sources.

Parameters	SECRAL-II	SECRAL
ω_{rf} (GHz)	18–28	18–24
Axial field peaks (T)	3.7/2.2	3.7/2.2
Mirror length (mm)	420	420
No. of axial SNs	3	3
B_r at chamber inner wall (T)	2.0	1.8
Coldmass length (mm)	~810	~810
SC-material	NbTi	NbTi
Magnet cooling	LHe bathing	LHe bathing
Warm bore ID (mm)	142.0	140.0
Chamber ID (mm)	125.0	120.5

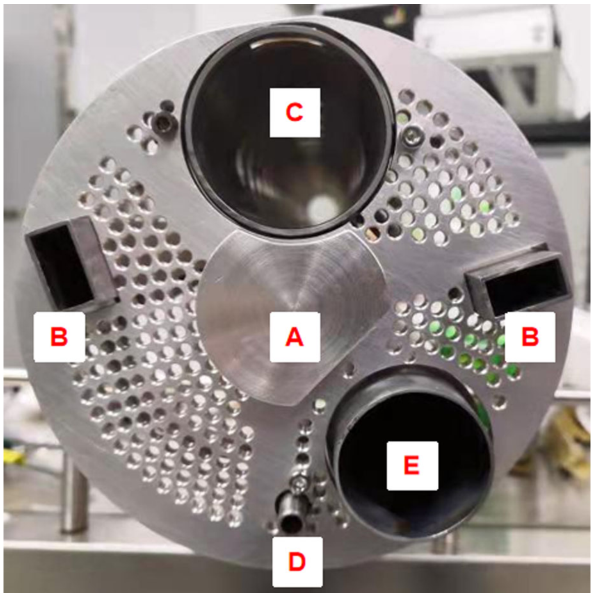

FIG. 3. Plasma chamber injection system of SECRAL-II ion source. The biased disc (A) is at the center, surrounded on both sides by two WR62 type rectangular waveguides (B). The oven port (C) is at the top and the gas inlet (D) is at the bottom. The circular waveguide is located in place (E).

maximum output power of 1.5 kW, and both the two waveguides were equipped with high voltage break and vacuum window. A digital delay and pulse generator, Quantum 9520 Series, was used to generate transistor-transistor logic (TTL) input signals allowing to drive the gyrotron and klystron pulsed operation as well as varied pulse patterns that can be used to modulate the temporal synchronization between the two microwave sources. The leading or trailing edge of the microwave pulse signal is typically less than 1 μs, and the precision of timing adjustment for the microwave pulse is better than 0.01 ms, which is adequate for our study. The ion beam currents were measured across a 1 kΩ resistor directly connected to the Faraday cup situated after the beam analyzing magnet. An oscilloscope was used to display and record the temporal structures of the microwave pulse signal and beam current signal. The schematic of the experimental setup is shown in Fig. 4.

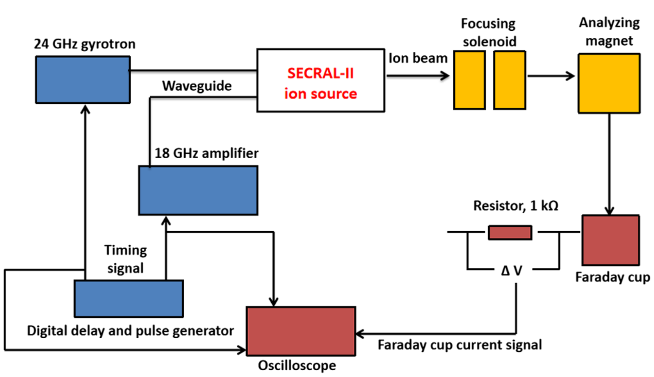

FIG. 4. Schematic figure of the experimental setup.

III. EXPERIMENTAL RESULTS

Metallic beam production is tricky, and the performance could be easily affected by many aspects such as the oven condition, incident metal sample, plasma chamber conditioning, and so on. To facilitate the experiment, the heavy gaseous element xenon is adopted. In all measurements, the ion source was operated with xenon plasma and tuned for high charge state (30+ to 42+) xenon ion production. The typical extraction voltage was 20 kV at a total power level of 8 kW and the repetition rate of the two microwave sources was set to 2 Hz. A previous study [12] indicates that the temporal synchronization between two microwave sources is a key parameter affecting plasma decay and afterglow characteristic, so in the first part of this study, the primary microwave (24 GHz) pulse width and other tuning parameters were first optimized to stabilize the extracted beam currents and then kept constant, the secondary microwave (18 GHz) pulse width was changed for a parameter study. For Xe^{34+} production, the 24-GHz microwave pulse width was set to 250 ms and the 18-GHz microwave pulse width was changed from 245 to 255 ms. The experiment results (Fig. 5) show that when the pulse width of an 18-GHz microwave is shorter (up to 5 ms) than the pulse width of a 24-GHz microwave, it does not have a pronounced influence on both the peak current and decay time of the afterglow waveform. Conversely, the afterglow waveform is significantly modulated when the pulse width of 18-GHz microwave is 1.5–2 ms longer than that of the 24 GHz, both the afterglow peak current and decay time are dramatically reduced in this condition. On the other hand, a further increase of the 18-GHz microwave pulse width (from 252 to 255 ms) has no more effect on the afterglow waveform. Detailed waveform parameters and peak current are shown in Table II and Fig. 6, it is clearly shown that the maximum peak current and decay time are obtained when the pulse widths of the two microwave sources are almost identical. This conclusion was also confirmed with Xe^{30+} and Xe^{38+}.

As the second part of this study, for optimization of the afterglow beam currents, following the experimental results obtained in the first part as presented in the afore contents, the ion source was operated with two microwave sources at

TABLE II. Detailed waveform parameters of Xe^{34+} afterglow beams.

Ion	Pulse width of 18-GHz microwave (ms)	Rise time (ms)	$1/e$ decay time (ms)
Xe^{34+}	245	3.73	8.59
	250	3.59	10.35
	252	2.20	2.68

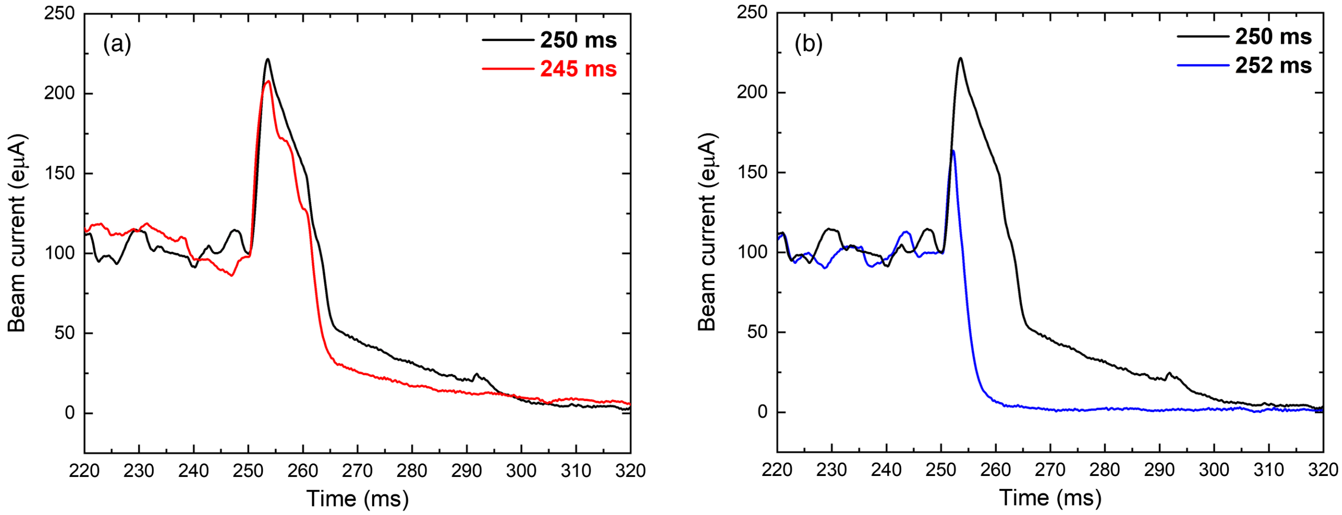

FIG. 5. Afterglow waveform of Xe^{34+} with varied 18-GHz microwave pulse width. The black line presents the waveform with a 250 ms pulse width of an 18-GHz microwave. The red and blue lines present the waveform with 245 ms (a) and 252 ms (b) pulse widths of an 18-GHz microwave. The microwave power of 24 GHz and 18 GHz are 7.0 and 0.7 kW, respectively.

the same pulse widths. The main tuning parameters were microwave pulse width, magnetic field, gas pressure, and biased disk voltage. It is found that the optimum microwave pulse width increases with the increasing charge state (shown in Fig. 7). Meanwhile, the production time and saturation time of highly charged ions also increase with the charge state (see Fig. 8). For example, the beam intensity is seen by the Faraday cup at 22 ms for Xe^{30+} and 91 ms for Xe^{42+} and then saturates at 75 and 280 ms, respectively. In addition, the optimum magnetic fields in afterglow mode are higher than those used in cw mode: in the case of Xe^{34+}, the optimum magnetic fields in cw mode are $B_r = 1.79$ T, $B_{inj} = 3.07$ T, $B_{min} = 0.55$ T, and $B_{ext} = 1.72$ T, and in afterglow mode, the optimum magnetic fields are $B_r = 1.84$ T, $B_{inj} = 3.08$ T, $B_{min} = 0.64$ T, and $B_{ext} = 1.89$ T. This observation is consistent with an experimental study with the CERN GTS-LHC ECR ion source [12] and suggests that SECRAL-II could be a very good trap in which very high charge states are accumulated before release when the microwave power is stopped.

It is encouraging to see from Table III that the optimum peak currents obtained during the afterglow mode are much higher than the beam intensity records obtained in cw mode. Compared with SECRAL ion source operated at the same frequency (24 + 18 GHz) and power (~8 kW), the beam intensity of highly charged xenon ions in afterglow mode is 1.4–4.2 times higher than those in cw mode, even compared with the beam intensity records of SECRAL-II

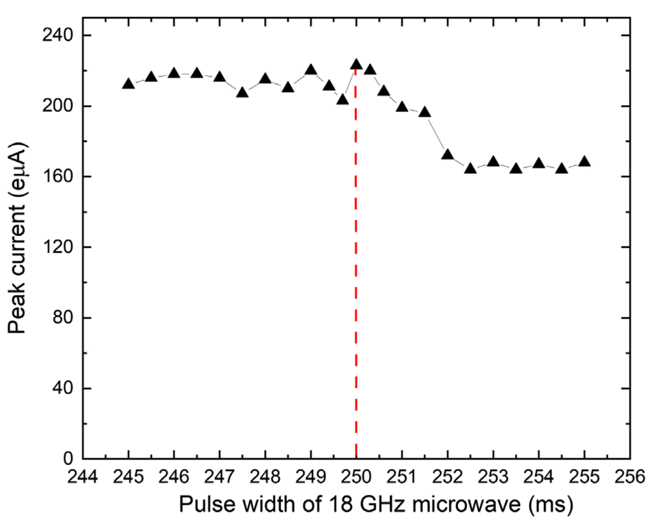

FIG. 6. Peak current of Xe^{34+} afterglow beams with varied 18-GHz microwave pulse width. The pulse width of the 24-GHz microwave is set to 250 ms.

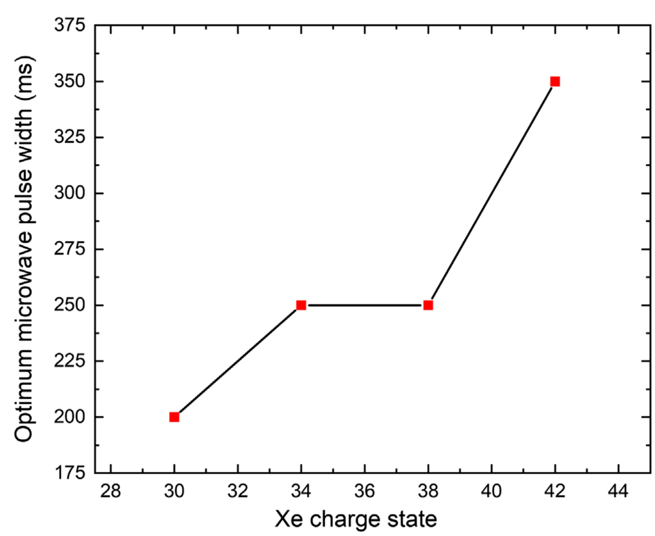

FIG. 7. Evolution of the optimum microwave pulse width with xenon charge states.

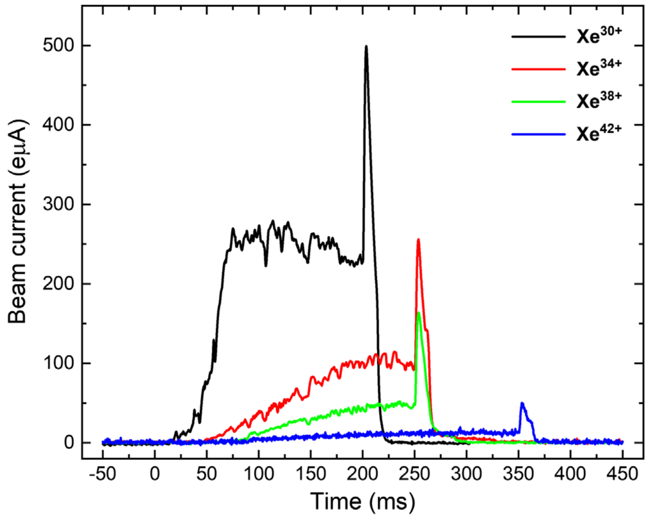

FIG. 8. The optimum afterglow beams for different xenon charge states. The microwave power is turned on at 0 ms.

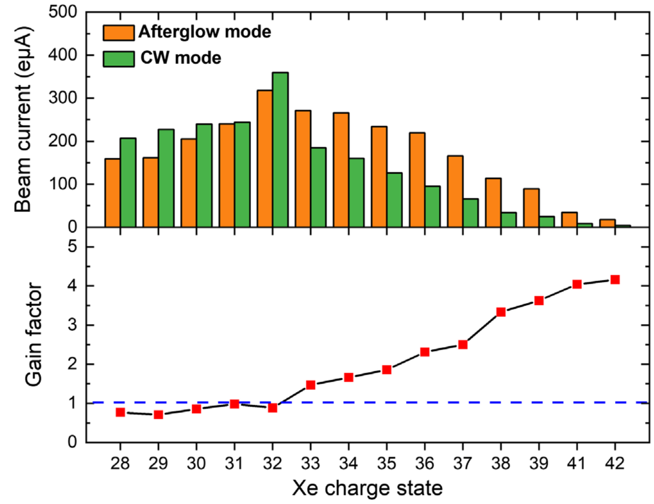

FIG. 9. Xenon charge state distributions for cw mode and afterglow mode optimized on Xe^{34+}, in this figure, Xe^{32+} overlaps with O^{4+} and Xe^{40+} with O^{5+}. To illustrate a clearer variation trend of beam intensity, Xe^{40+} is not shown in this figure. In addition, the gain factor of beam intensity in afterglow mode compared to cw mode is presented.

obtained at higher microwave frequency (28 + 18 GHz) and higher power (~10 kW), the gain factor is also up to ~3. Figure 9 shows xenon charge state distributions (CSDs) optimized for Xe^{34+} at cw mode and afterglow mode. The gain factor of beam intensity in optimized afterglow mode compared to optimized cw mode is greater than 1 for those ion beams with the charge states above the peak current CSD in cw mode, i.e., Xe^{31+} and increases with the charge state. Furthermore, detailed waveform parameters shown in Table IV indicate that the peak duration (duration of beam current exceeding 90% of peak current) is greater than 2 ms, which can sufficiently fulfill the requirement of the HIAF project.

IV. DISCUSSION

The experimental results obtained in the first part indicate that the maximum peak intensity is obtained when the pulse widths of the two microwave sources are almost identical. Based on experimental measurement [20] and theoretical consideration [21], it has been suggested that highly charged ions are originating from the central region of the plasma and trapped in an electrostatic potential dip created by the electron population, the confinement of the ions is therefore affected by the magnitude of the potential dip. In afterglow mode when the microwave power is turned off, a fraction of cold electrons would immediately escape the plasma due to the removal of the "ECR-plug" effect [22], i.e., interruption of electron heating populating the electron loss cone. The sudden escape of cold electrons would cause the potential dip to diminish, decreasing the ion confinement and releasing highly charged ions from the trap. As we know double frequency heating creates two closed ECR surfaces on which cold electrons will be heated and the secondary resonance zone is enclosed by the primary resonance, when the secondary frequency (18 GHz in our study) is turned off before the primary one (24 GHz), a fraction of cold electrons will escape from the trap and the dip is presumably affected; however, as the outer ECR surface created by the primary frequency still exists, these escaping electrons could be effectively heated by the primary frequency and again constrained during their loss process and eventually escape with the switch-off of the primary power source, which is then observed as a slight decrease in the extracted beam currents [shown in

TABLE III. Comparison of xenon beam intensity records between cw and afterglow mode on SECRAL and SECRAL-II ion sources (beam intensity: eμA).

Ion	SECRAL 24 + 18 GHz (~8 kW cw)	SECRAL-II 28 + 18 GHz (~10 kW cw)	SECRAL-II 24 + 18 GHz (~8 kW AG)
Xe^{30+}	360	400	503
Xe^{34+}	120	160	266
Xe^{38+}	23	56	169
Xe^{42+}	12	16	50

TABLE IV. Waveform parameters of optimum xenon afterglow beams.

Ion	Rise time (ms)	$1/e$ decay time (ms)	Peak duration (ms)
Xe^{30+}	3.53	10.18	2.83
Xe^{34+}	3.46	10.40	2.37
Xe^{38+}	3.35	9.65	2.80
Xe^{42+}	3.15	10.45	2.44

Fig. 5(a)]. Conversely, when the secondary frequency is turned off after the primary one, it keeps a fraction of the electron (and ion) population trapped inside the chamber and does not release them with the switch-off of the primary power source, which leads to a significant decrease in the extracted peak beam currents [shown in Fig. 5(b)]. To diminish the potential dip and release highly charged ions as much as possible, the two microwave sources should be turned off simultaneously.

The $1/e$ decay time in our study with double frequency heating is much longer than that obtained on a second generation ECR ion source (~2 ms) operated at 14.5-GHz microwave frequency and corresponding lower magnetic field strength [8]. Theoretical research [22] suggests that the evolution of the ion density n_α during the afterglow discharge can be written as

$$n_\alpha = n_{\alpha 0} e^{-t/\tau} = n_{\alpha 0} e^{-D_\alpha t/C}, \tag{1}$$

where $n_{\alpha 0}$ is the initial ion density at the moment of microwave turn-off, τ is the characteristic $1/e$ decay time, D_α is the diffusion constant, and C depends on the characteristic dimension of ion trapping (plasma dimension). It can be deduced from Eq. (1) that the characteristic $1/e$ decay time is proportional to the plasma dimension but inversely proportional to the diffusion constant. A previous study [13] indicates that the diffusion process in afterglow transient is probably Bohm diffusion and the semiempirical equation for the diffusion constant is of the form

$$D_{\mathrm{Bohm}} = \frac{kT_e}{16eB}, \tag{2}$$

where kT_e is the electron temperature, e is the elementary charge, and B is the (average) magnetic field strength. Equations (1) and (2) suggest that the decay time of the afterglow transient is proportional to the magnetic field strength. To further investigate the effects of the magnetic field strength and plasma volume, the decay time of Xe^{30+} beams was measured at 18, 24, and 24 + 18 GHz, respectively. In this measurement, the axial and radial mirror ratios are scaled to the primary heating frequency and kept identical in each case (see Table V), as a result, the plasma volume enclosed by the cold electron resonance is approximately constant under this condition. It is found that the decay time is insensitive to the microwave power, for 24-GHz heating frequency when the microwave power is changed from 1 to 7 kW, the variation of the decay time is less than 6% (from 12.41 to 11.68 ms). More importantly, the experimental results shown in Table V indicate that when the plasma volume is constant, the decay time for different microwave frequencies is almost proportional to the magnetic field strength. On the other hand, the decay time measured at 18-GHz microwave frequency in our measurement is still ~4 times longer than that in Ref. [8], but the corresponding magnetic field strength is less than 2 times higher than that operated at 14.5-GHz microwave frequency, which implies that the magnetic field strength alone does not determine the decay time. For SECRAL-II ion source, the plasma volume enclosed by the cold electron resonance, V_{ECR}, is about 2–3 times larger than a second generation ECR ion source [23], based on the above analyses, it may be argued that the plasma volume also plays an important role in determining the decay time and the longer decay obtained in our study is most likely a combined effect of stronger magnetic field and larger plasma volume, an intrinsic feature of a third generation ECR ion source operating typically at 24–28 GHz.

TABLE V. Comparison of key parameters of Xe^{30+} afterglow beams with different microwave frequencies. The volume enclosed by the cold electron resonance, V_{ECR}, is estimated by considering the resonance zone as a 3D ellipsoid surface and the microwave power is 1 kW for each case.

Frequency (GHz)	$B_\mathrm{r}(T)$	$B_\mathrm{inj}(T)$	$B_\mathrm{min}(T)$	$B_\mathrm{ext}(T)$	V_{ECR} (cm^3)	Decay time (ms)
24 + 18	1.83	3.32	0.69	2.02	422	11.76
24	1.83	3.32	0.69	2.02	422	12.41
18	1.37	2.49	0.52	1.52	423	8.72

In addition, it is found that the production time of highly charged ions increases with the charge state (from 22 ms of Xe^{30+} to 91 ms of Xe^{42+}), and this finding is consistent with an experimental study [24], in which it was concluded that the production time of highly charged ions in ECRIS plasmas is several tens of ms and increases with the charge state. Meanwhile, the saturation time of highly charged ions is several hundreds of ms (e.g., 205 ms of Xe^{38+} and 280 ms of Xe^{42+}), which is much longer than that on a second generation ECR ion source (usually less than 100 ms) [8]. This suggests that it takes a longer time for highly charged ions to reach a stable equilibrium when operating a third generation superconducting ECR ion source with a larger plasma chamber at high frequency and high power, and consequently long microwave pulse length is needed for the optimization of afterglow beam currents.

Generally, the present work reports for the first time (to our knowledge) that intense pulsed beams of highly charged ions with long peak duration (greater than 2 ms) could be produced by operating a third generation ECR ion source in afterglow mode with double frequency heating. Both the peak current and duration are controllable by manipulating the incident microwave power generators. This study provides a viable option for the HIAF project: adequate peak duration could meet the requirement of the two-plane painting multiturn injection scheme and thus high injection gain could be achieved in HIAF BRing, and meanwhile, the large gain of beam intensity obtained in afterglow mode could directly and significantly enhance the performance of synchrotron. These features will have a fundamental impact on the performance of heavy ion synchrotron accelerators. Moreover, this work also indicates that it is most likely to further improve the afterglow performance by operating a fourth generation ECR ion source operating at an even higher frequency (≥45 GHz) and higher power (≥20 kW). Nevertheless, the precise modulation of the afterglow waveform at high frequency and high power will be a topic of future investigations with the state-of-the-art ECR ion sources.

ACKNOWLEDGMENTS

The authors wish to thank O. Tarvainen, V. Toivanen, and H. Koivisto of JYFL for helpful guidance and discussion. This work has been supported by the CAS (Contract No. GJJSTD20210007) and the NSFC (Contracts No. 12025506, No. 11427904, and No. 12175285).

[1] J. C. Yang, J. W. Xia, G. Q. Xiao, H. S. Xu, H. W. Zhao, X. H. Zhou, X. W. Ma, Y. He, L. Z. Ma, D. Q. Gao *et al.*, HIAF (High Intensity Heavy Ion Accelerator Facility) in China, Nucl. Instrum. Methods Phys. Res., Sect. B **317**, 263 (2013).

[2] L. P. Yao, W. P. Chai, J. C. Yang, J. W. Xia, G. D. Shen, J. Li, J. Liu, H. Ren, S. Ruan, G. Wang, Z. Q. Dong, and F. C. Cai, Beam-loss driven injection optimization for HIAF-BRing in the presence of space charge, Nucl. Instrum. Methods Phys. Res., Sect. A **951**, 162876 (2020).

[3] X. Q. Chen, J. C. Yang, J. W. Xia, G. D. Shen, S. Ruan, G. Wang, J. Liu, J. J. Zhang, and F. C. Cai, Study of eddy current effect in BRing at HIAF, Nucl. Instrum. Methods Phys. Res., Sect. A **920**, 37 (2019).

[4] H. W. Zhao, L. T. Sun, J. W. Guo, W. H. Zhang, W. Lu, W. Wu, B. M. Wu, G. Sabbi, M. Juchno, A. Hafalia, E. Ravaioli, and D. Z. Xie, Superconducting ECR ion source: From 24–28 GHz SECRAL to 45 GHz fourth generation ECR, Rev. Sci. Instrum. **89**, 052301 (2018).

[5] G. Melin, F. Bourg, P. Briand, J. Debernardi, M. Delaunay, R. Geller, B. Jacquot, P. Ludwig, T. K. N'Guyen, L. Pin, M. Pontonnier, J. C. Rocco, and F. Zadworny, Some particular aspects of the physics of the ECR sources for multicharged ions, Rev. Sci. Instrum. **61**, 236 (1990).

[6] C. E. Hill and K. Langbein, Experiments on a 14.5 GHz electron cyclotron resonance source, Rev. Sci. Instrum. **69**, 643 (1998).

[7] C. E. Hill, D. Küchler, R. Scrivens, D. Hitz, L. Guillemet, R. Leroy, and J. Y. Pacquet, GTS-LHC: A new source for the LHC ion injector chain, AIP Conf. Proc. **749**, 127 (2005).

[8] K. Tinschert, R. Iannucci, J. Bossler, and R. Lang, Experimental studies of the afterglow mode with xenon in a CAPRICE ECRIS, Rev. Sci. Instrum. **75**, 1407 (2004).

[9] L. Maunoury, L. Adoui, J. P. Grandin, F. Noury, B. A. Huber, E. Lamour, C. Prigent, J. P. Rozet, D. Vernhet, P. Leherissier, and J. Y. Pacquet, Afterglow mode and the new micropulsed beam mode applied to an electron cyclotron resonance ion source, Rev. Sci. Instrum. **79**, 02A313 (2008).

[10] P. Sortais, Pulsed ECR ion source using the afterglow mode, Rev. Sci. Instrum. **63**, 2801 (1992).

[11] M. Kidera, M. Lamoureux, V. Mironov, T. Nakagawa, and G. Shirkov, Correlation between the hot-electron dynamics and the afterglow currents in electron cyclotron resonance ion sources, Rev. Sci. Instrum. **70**, 4234 (1999).

[12] V. Toivanen, G. Bellodi, D. Küchler, F. Wenander, and O. Tarvainen, Effect of double frequency heating on the lead afterglow beam currents of an electron cyclotron resonance ion source, Phys. Rev. Accel. Beams **20**, 103402 (2017).

[13] O. Tarvainen, T. Ropponen, V. Toivanen, T. Kalvas, J. Ärje, and H. Koivisto, Diagnostics of plasma decay and afterglow transient of an electron cyclotron resonance ion source, Plasma Sources Sci. Technol. **19**, 045027 (2010).

[14] L. Sun, J. W. Guo, Z. Shen, W. H. Zhang, X. Z. Zhang, W. Lu, L. B. Li, Y. Yang, X. Fang, H. Y. Ma, Y. C. Feng, W. Huang, J. J. Chang, P. P. Wang, D. Hitz, and H. W. Zhao, Technical approaches towards intense high charge state ion beam production with superconducting ECRIS, AIP Conf. Proc. **2011**, 040022 (2018).

[15] L. Sun, W. Lu, W. Wu, T. J. Yang, Y. Yang, B. M. Wu, E. M. Mei, S. J. Zheng, D. S. Ni, B. Zhao, L. Zhu, Q. Hu, M. Z. Guan, W. H. Zhang, J. W. Guo, X. Fang, X. Z. Zhang, H. W. Zhao, and L. Z. Ma, Status report of SECRAL II ion source development, in *Proceedings of the 21st International Workshop on ECR Ion Sources, Nizhny Novgord* (JACoW, 2014), p. 94.

[16] H. W. Zhao, Z. M. Zhang, W. He, X. Z. Zhang, X. H. Guo, Y. Cao, P. Yuan, L. T. Sun, L. Ma, M. T. Song, W. L. Zhan, B. W. Wei, and D. Z. Xie, Intense heavy ion beam production from IMP LECR3 and construction progress of a superconducting ECR ion source SECRAL, Rev. Sci. Instrum. **75**, 1410 (2004).

[17] H. W. Zhao, L. T. Sun, X. Z. Zhang, Z. M. Zhang, X. H. Guo, W. He, P. Yuan, M. T. Song, J. Y. Li, Y. C. Feng, Y. Cao, X. X. Li, W. L. Zhan, B. W. Wei, and D. Z. Xie, Advanced superconducting electron cyclotron resonance ion source SECRAL: Design, construction, and the first test result, Rev. Sci. Instrum. **77**, 03A333 (2006).

[18] H. W. Zhao, L. T. Sun, X. Z. Zhang, X. H. Guo, Y. Cao, W. Lu, Z. M. Zhang, P. Yuan, M. T. Song, H. Y. Zhao, T. Jin, Y. Shang, W. L. Zhan, B. W. Wei, and D. Z. Xie, Intense beam production of highly charged heavy ions by the superconducting electron cyclotron resonance ion source SECRAL, Rev. Sci. Instrum. **79**, 02A315 (2008).

[19] H. W. Zhao, L. T. Sun, J. W. Guo, W. Lu, D. Z. Xie, D. Hitz, X. Z. Zhang, and Y. Yang, Intense highly charged ion beam production and operation with a superconducting electron cyclotron resonance ion source, Phys. Rev. Accel. Beams **20**, 094801 (2017).

[20] P. Spädtke, K. Tinschert, R. Lang, J. Mäder, J. Roßbach, J. W. Stetson, and L. Celona, Prospects of ion beam extraction and transport simulations, Rev. Sci. Instrum. **79**, 02B716 (2008).

[21] V. P. Pastukhov, Classical longitudinal plasma losses from open adiabatic traps, Rev. Plasma Phys. **13**, 203 (1987).
[22] R. Geller, *Electron Cyclotron Resonance Ion Sources and ECR Plasmas* (IOP Publishing Ltd., London, 1996).
[23] V. A. Skalyga, I. V. Izotov, A. G. Shalashov, E. D. Gospodchikov, E. M. Kiseleva, O. Tarvainen, H. Koivisto, and V. Toivanen, Controlled turbulence regime of electron cyclotron resonance ion source for improved multicharged ion performance, J. Phys. D **54**, 385201 (2021).
[24] R. C. Vondrasek, R. H. Scott, R. C. Pardo, and D. Edgell, Techniques for the measurement of ionization times in ECR ion sources using a fast sputter sample and fast gas valve, Rev. Sci. Instrum. **73**, 548 (2002).